Pergamon

PII: S0277-5387(97)00128-9

Polyhedron Vol. 16, No. 21, pp. 3835–3846, 1997

0277–5387/97 $17.00+0.00

Equilibria of chromate(VI) species in acid medium and *ab initio* studies of these species

F. Brito,[a]* J. Ascanio,[a] S. Mateo,[a] C. Hernández,[a] L. Araujo,[a] P. Gili,[b]* P. Martín-Zarza,[b] S. Domínguez[b] and A. Mederos[b]

[a] Grupo de Equilibrios en Solución, Escuela de Química, Facultad de Ciencias, Universidad Central de Venezuela (UCV), Caracas, Venezuela

[b] Departamento de Química Inorgánica, Facultad de Farmacia, Universidad de La Laguna (ULL), Tenerife, Canary Islands, Spain

(Received 18 December 1996; accepted 2 April 1997)

Abstract—The study of the H^+–CrO_4^{2-} system in 3.0 M KCl as ionic medium at 25°C by means of *emf* (glass electrode) and direct calorimetric measurements, in the total Cr^{VI} concentration (B), average number of H^+ bounds per central group CrO_4^{2-} (Z), and pH ranges: $25 \leqslant B \leqslant 100$ mM, $0 \leqslant Z \leqslant 1.16$ and $1 \leqslant pH \leqslant 8$, respectively, indicates the formation of the following complexes $H_p(CrO_4)_q^{(p-2q)}$, stability constants ($\log \beta_{pq}(\pm 3\sigma)$) and partial molar enthalpies ($\Delta H_{pq}(\pm 3\sigma)$ kcal.mol^{-1}): $HCrO_4^-$, 5.888(4), −0.6(1); $Cr_2O_7^{2-}$, 13.900(3), −5.7(1); H_2CrO_4, 7.004(7), 1.8(2) and $HCr_2O_7^-$, 15.007(5), −5.0(1), respectively, according to the general reaction: $pH^+ + qCrO_4^{2-} \rightleftarrows H_p(CrO_4)_q^{(p-2q)}$. The results previously obtained by Raman spectroscopy for this system are better adjusted when the $HCrO_4^-$ species is included. The energies and optimized structures from *ab initio* calculations for the CrO_4^{2-}, $HCrO_4^-$, $Cr_2O_7^{2-}$, H_2CrO_4 and $HCr_2O_7^-$ species have also been obtained. For the $HCrO_4^-$ species the values of bond lengths and angles theoretically calculated are in good agreement with the experimental data of the anion in the crystal structure of the compound $(PPh_4)[Cr^{VI}O_3(OH)]$. Finally, correlations between thermodynamic experimental and structural theoretical parameters are discussed. © 1997 Elsevier Science Ltd

Keywords: stability constants; chromate; hydrogen chromate; dichromate; hydrogen dichromate; *ab initio* calculations.

Over the last few years, there has been a renewed interest in the study of the chromate–dichromate system in relation to the formation of chromium(VI)–thioester [1] and chromium(VI)–glutathione [2] compounds, which may be involved in the important role of the carcinogenicity and mutagenicity of chromium(VI). In the process of formation of the quoted compounds, the $HCrO_4^-$ species is implicated. This species is well known in textbooks [3,4]. However, in references [5–7], examining the Raman spectra of chromates, dichromates and chlorochromates in aqueous solution, in the ranges of pH and total chromium(VI) concentration (B) $11 \geqslant pH \geqslant 1$ and $300 \geqslant B \geqslant 3$ mM, the authors deduce that the protonated form of chromate $HCrO_4^-$ does not exist, although in accordance with a more recent publication [8], these results need to be reconfirmed by other methods. In reference [9], studying the electronic spectra of aqueous chromium(VI) solutions in the pH range 3–11, the authors conclude that $HCrO_4^-$ is spectrophotometrically undetectable. However, Palmer *et al.* [10] have convincingly argued the formation of $HCrO_4^-$ from high-pressure, high-temperature Raman studies and new evidences for the existence of the $HCrO_4^-$ anion have been reported by other authors [11]. Moreover, recently in reference [12] the crystal structure of $(Ph_4P)[Cr^{VI}O_3(OH)]$ has been described. In a recent review these disagreements are treated [13].

We have been working for a long time on this question. Also, considerable uncertainty exists about the nature of the orange–red chromium(VI) species [14,15], which can occur in very acidic solutions: H_2CrO_4 and/or $HCr_2O_7^-$.

Chromium(VI) does not give rise to the extensive

* Authors to whom correspondence should be addressed.

and complex series of iso- and heteropolyanions characteristic of the somewhat less acidic oxides of V^V, Mo^{VI} and W^{VI}, perhaps due to the greater extent of multiple bonding (Cr=O) for the smaller chromium ion [3,16], although the Cr—O bond also has ionic character [17]. Moreover, in basic solutions above pH 8 the main species is the tetrahedral yellow chromate ion CrO_4^{2-}; in the range $6 \geqslant pH \geqslant 2$, $HCrO_4^-$ and the orange-red dichromate ion $Cr_2O_7^{2-}$ are in equilibrium; and at pHs below 1 the main species is H_2CrO_4. The equilibria are represented by the following pK values: 0.6 and 5.9, as well as the dimerization constant $k_{22} = 159$ for the reaction (1).

$$2HCrO_4^- \rightleftarrows Cr_2O_7^{2-} + H_2O \qquad (1)$$

Chemical shifts in the ^{17}O NMR absorptions for the bridging and terminal oxygen of $Cr_2O_7^{2-}$, and for $HCrO_4^-$ present at equilibrium with $Cr_2O_7^{2-}$, has been reported [18]. The broadening of the former signals, and that for the water solvent caused by adding acid were interpreted as arising from the operation of equilibrium (1) catalized by H^+. In addition, there are several hydrolysis equilibria which have been studied kinetically [16,19]. For reaction (1) the rate constant from left to right is about 2 M^{-1} sec^{-1} and for the basic hydrolysis of $Cr_2O_7^{2-}$ by H_2O and OH^-, which are first order in both dichromate and base concentration, the rate constants have values around 5×10^{-5} and 400 M^{-1} sec^{-1}, respectively. Therefore, the behaviour of the Cr^{VI} in solution is simpler than other group VI elements, which form polyoxometalates [20] with 7 Mo or 6 W, whose mechanisms of formation are unknown [16].

Whether chromates or dichromates crystallize depends on the pH, the total metal concentration and the cation present. The tetrahedral structure of the anion CrO_4^{2-} has been confirmed by many single X-ray studies. Within the CrO_4^{2-} groups the O—Cr—O angles are close to the tetrahedral value and the Cr—O bond distances are essentially equal and close to 1.6 Å. The anion $Cr_2O_7^{2-}$ consisted of two distorted CrO_4 tetrahedra [16,17,21] with a corner in common; the bridging Cr—O distance is close to 1.8 Å, while the terminal Cr—O bonds are similar to those in CrO_4^{2-}, and the Cr—O—Cr angles are around 122–139°. In very strong acid media, high chromium(VI) concentrations: 4 and 12.5 M, and large $CrO_3/Cr_2O_7^{2-}$ molar ratios: 8.6 and 92.5, respectively, crystalline trichromates and tetrachromates are formed and the structures contain $Cr_3O_{10}^{2-}$ and $Cr_4O_{13}^{2-}$ ions composed of three and four CrO_4 tetrahedra, continue the pattern set by the $Cr_2O_7^{2-}$ ion in having chains of CrO_4 tetrahedra sharing corners [22,23]. At the limit is the CrO_3 oxide, which consist of infinite chains [3] of —O—CrO_2—O— corner-sharing tetrahedra. The Raman spectra confirm in very acidic solutions the presence of tri- and tetrachromates [6,7].

On the other hand, since the initial Wolfsberg and Helmholz's studies of the electronic structure of tetraoxocomplexes of transition metals with a closed shell [24], several inorganic and organometallic compounds have been the subject of extensive theoretical investigations [25]. However, for the protonated species derived from the CrO_4^{2-} and $Cr_2O_7^{2-}$ anions, we have not found any previous references in the literature, with the exception [26] of $HCrO_4^-$, on energies and optimized structures obtained from *ab initio* calculations. Ozeki *et al.* [27] studied the structures of CrO_4^{2-}, $HCrO_4^-$, H_2CrO_4 and $Cr_2O_7^{2-}$ in aqueous solution using the UV–vis absorption spectra and optimizing these structures so that UV–vis absorption spectra reproduced from molecular orbital calculation DV-Xα are fitted to the experimentally obtained component spectra.

We now analyse the studies carried out in aqueous solution, where CrO_4^{2-} ion gives polynuclear acid complexes $H_p(CrO_4)_q^{(p-2q)-}$, in the following denoted for brevity by the set (p, q), according to the general reaction (2).

$$pH^+ + qCrO_4^{2-} \rightleftarrows H_p(CrO_4)_q^{(p-2q)} \qquad (2)$$

So then, we have for chromium and hydrogen ions the mass balance eqs (3).

$$B = b + \Sigma\Sigma q c_{pq}$$

$$BZ(= H - h + K_w h^{-1}) = \Sigma\Sigma p c_{pq} \qquad (3)$$

Chemical symbols are in roman and concentrations in *italic* type [28]. H and B represent the total analytical concentrations of H^+ and metal, and h, b and c_{pq} are the equilibrium concentrations of H^+, CrO_4^{2-} and complex (p, q), respectively; K_w is the water dissociation constant, and Z is defined as the average number of H^+ bounds per central (metal) group CrO_4^{2-} [28,29]. Concentrations and equilibrium constants are expressed in M (moles per litre) and errors are parenthetically given [30].

The first study of the acidification of chromates(VI) in solution using the *inert ionic medium* method [31–35] was accomplished by Sasaki [15], who made *emf* (glass electrode) and spectrophotometric UV-vis (374, 390 and 400 nm) measurements in 3.0 M $NaClO_4$ at 25°C, for the total chromium(VI) concentrations interval $1 \leqslant B \leqslant 200$ mM, covering the range $0 \leqslant Z \leqslant 1.17$. For $Z < 1$, as it increases, the experimental family of curves $Z(pH, B)$ shift as B and pH ($= -\log h$) also increase, which indicates that toward $Z = 1$, polymerization reactions take place and at least one *polynuclear* complex forms, since all curves for various chromium(VI) total concentrations do not coincide. Therefore, in the wide range with $Z \sim 1$, the predominating species must have the general formula $(HCrO_4)_q^{q-}$. Moreover, in contrast to the above-mentioned authors [5–7], one of these complexes must be $HCrO_4^-$, since for low B the curves are seen to approach to the so called *mononuclear wall* [36], which has the right shape to correspond to equilibrium of CrO_4^{2-} and $HCrO_4^-$. Thus, Sasaki [15] confirmed the

Table 1. Stability constants and partial molar enthalpies for the reactions (1) and (2) at 25°C

(p,q)	Medium	Reaction	$\log\beta_{pq}$	ΔH_{pq} (kcal/mol)	Ref.
(1,1)	3 M $Na(ClO_4)$	(2)	5.89(2)	1.08(9)	[15,46]
(2,2)		(2)	13.98(4)	−2.68(4)	[15,46]
		(1)	2.20(2)	−4.8(1)	[15,46]
(1,1)	3 M K(Cl)	(2)	5.91(1)	−0.6(2)	[28,35]
(2,2)		(2)	13.87(3)	−5.7(1)	[28,35]
		(1)	2.05(5)	−4.5(5)	[28,35]
	3 M $NaNO_3$	(1)	2.16		[14]
(1,1)	dil	(2)		0.7(4)	[48,49]
(2,2)		(1)		−4.7(3)	[48,49]

presence of the $HCrO_4^-$ and $Cr_2O_7^{2-}$ complexes, not finding any evidence of other products being detected at pH > 1.5. Using graphical methods, the values of the stability constants $\log\beta_{pq}(3\sigma)$ obtained by this author were $\log\beta_{11} = 5.89(1)$, $\log\beta_{22} = 13.98(4)$ and $\log k_{22} = 2.20(2)$ (Table 1). On the other hand, by using *least-squares* methods (program Letagrop, *vide infra*) for the *emf* data of Sasaki [15], we obtained the values $\log\beta_{11} = 5.903(4)$, $\log\beta_{22} = 14.009(6)$ and $\log k_{22} = 2.20(1)$, with a standard deviation $\sigma(Z) = 0.004$, in good agreement with that stability constants, while only assuming the complex $Cr_2O_7^{2-}$ according to references [5–7], we obtain $\log\beta_{22} = 14.36(6)$, with a standard deviation $\sigma(Z) = 0.065$. Hence, for the *emf* data of Sasaki [15] the model containing the species $HCrO_4^-$ and $Cr_2O_7^{2-}$ gives much better fit than the one only assuming the dimer $Cr_2O_7^{2-}$. However, at high acidities, Z goes beyond 1, reaching the limit values $Z = 1.2$ and pH 0.3, such that some new acid products besides $HCrO_4^-$ and $Cr_2O_7^{2-}$ must be formed. Nevertheless, since the small data accuracy due to the high acidity at which the measurements were carried out, in addition to the questionable functioning of the glass electrode in chromic acid solutions [34], it could not be confirmed whether the function Z(pH) was independent of B in this range. In any case, Sasaki [15] proposed two options, namely, the complexes $HCr_2O_7^{2-}$ with $\log\beta_{32} \leqslant 14.6$, or H_2CrO_4, with $\log\beta_{21} \leqslant 7.1$. Later on, other authors [14] carried out several studies of Cr(VI) in 0.5 and 1 M $NaClO_4$ at 25°C; from 1 to 7 M $NaClO_4$ at 20°C and from 1 to 7 M $NaNO_3$ at 25°C, in order to obtain more information about the influence of the ionic media and temperature on those reactions.

For that very reason, a few years ago we also studied the H^+—CrO_4^{2-} system using 3.0 M KCl as ionic medium, (a) in equilibrium, through *emf* measurements [35] (glass electrode, $1 \leqslant B \leqslant 100$ mM, $0 \leqslant Z \leqslant 1$) and by means of enthalpy titrations [37–40] (50 mM $\leqslant B \leqslant$ 200 mM, $0 \leqslant Z \leqslant 1.5$), respectively, at 25°C, and (b) kinetically, by concentration jump and *emf* chemical relaxation measurements [35–41] ($5 \leqslant B \leqslant 100$ mM, $0.2 \leqslant Z \leqslant 0.8$), at 25 and 5°C. The kinetics data should be discussed elsewhere [42].

The equilibrium data were analyzed using graphical methods [28,29], and by means of the Nernst/Leta [43,44] and Varm/Leta [45,46] versions of the generalized least-squares program Letagrop [47], respectively. This program searches for the combination of physicochemical parameters, such as stability constants β_{pq} or partial molar enthalpies ΔH_{pq}, as well as for the systematic errors in total (analytical) concentrations, etc., which respectively should do minimum the least-square sums $U = \Sigma(Z - Z^*)^2$ or $U = \Sigma(Q - Q^*)^2$, being Z^* and Q^*, the computed values using the proposed model.

First, the treatment of the earlier *emf* data [35] (Fig. 1) also only shows the formation of the species $HCrO_4^-$ and $Cr_2O_7^{2-}$. The values of the stability constants $\beta_{pq}(3\sigma)$ obtained were $\log\beta_{11} = 5.918(9)$, $\log\beta_{22} = 13.86(1)$ and $\log k_{22} = 2.02(3)$, with a standard deviation $\sigma(Z) = 0.004$ (Table 1). The continuous trace curves in Fig. 1 were calculated with

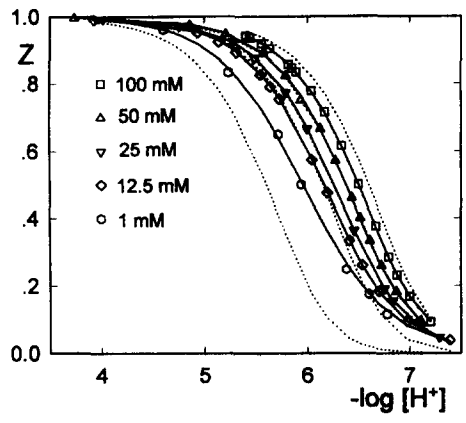

Fig. 1. Z, average number of H^+ bound per chromium(VI) at CrO_4^{2-} level *vs* pH at 25°C in 3.0 M KCl. The dotted lines were calculated assuming the species $Cr_2O_7^{2-}$ ($\log\beta_{22} = 14.2$, Refs. [5,6]) and the continuous lines were calculated assuming the species $HCrO_4^-$ and $Cr_2O_7^{2-}$ ($\log\beta_{11} = 5.918$, $\log\beta_{22} = 13.86$, Refs [38–42]).

this model. Like Sasaki's work, as Z increases, the experimental $Z(pH, B)$ data shift as B and pH also increase, which indicates that toward $Z = 1$ polymerization reactions take place, forming $(HCrO_4)_q^{q-}$ complexes. Also here, in contrast to the authors [5–7] already mentioned, one of these species must be $HCrO_4^-$, because for low B values the curves approach the *mononuclear wall* corresponding to the equilibrium between CrO_4^{2-} and $HCrO_4^-$ ions. The stability constant β_{11} is similar to Sasaki's value, but not β_{22} and k_{22}, whose values change only slightly with the ionic medium. Moreover, the dotted lines of Fig. 1 were calculated only assuming the formation of the complex $Cr_2O_7^{2-}$, according to references [5–7]. In this case, the value of the corresponding stability constant was $\log\beta_{22} = 14.2(1)$, with a standard deviation $\sigma(Z) = 0.068$. Therefore, also for these *emf* data [35], the model containing the complexes $HCrO_4^-$ and $Cr_2O_7^{2-}$ gives a much better fit than that one after the references [5–7] only assuming the dimer $Cr_2O_7^{2-}$.

Second, in the calorimetric studies [37–40] it was observed that for the $0 < Z < 1$ range the calorific effect was *exothermic*, while for Z or $H/B > 1$ (Fig. 2) it was *endothermic*. For the first Z interval the following partial molar enthalpies $\Delta H_{pq}(3\sigma)$ were obtained: $\Delta H_{11} = -0.6(1)$, $\Delta H_{22} = -5.7(1)$ and $\Delta H'_{22} = -4.7(5)$ kcal/mol [reaction (1)], which may be compared with Muldrow and Hepler's [48,49] and Arnek's [46] values compiled in Table 1. It may be observed that the dimerization heat of reaction (1) is practically independent of the ionic medium, while the formation of the complex $HCrO_4^-$ and $Cr_2O_7^{2-}$ is more exothermic in 3.0 M KCl than in the other media, so some kind of interaction between the chromate and the Cl^- ions [38] must be occurring, for example, the formation of CrO_3Cl^- ion [7,15,18].

The present work on the H^+–CrO_4^{2-} system gives account on the results of: (1) the analysis of a new series of *emf* data (glass electrode, 25°C, 3.0 M KCl, $25 \leqslant B \leqslant 100$ mM, $0 \leqslant Z \leqslant 1.16$) carried out in order to obtain more knowledge of the speciation topic for $Z > 1$, using the version Nernst/Leta [44] of Letagrop [47]; (2) the analysis of the earlier calorimetric endothermic experimental data quoted in [38,39] by means of the version Varm/Leta [45] of Letagrop [46]; (3) the analysis of the results previously obtained by Raman spectroscopy [5,6] using the version Beer/Leta [45,50] of Letagrop [47], which shows that the experimental data of the system H^+—CrO_4^{2-} fit better when the species $HCrO_4^-$ is included; (4) the study of the energetic stability of the protonated species of chromate(VI), using *ab initio* theoretical methods (SFC-MO), with double-zeta valence basis set, incorporating pseudopotentials with EPC (effective core potential) to take into account the internal electrons [51], in particular to study the influence of the protonation of oxygen in the CrO_4^{2-} and $Cr_2O_7^{2-}$ anion structure. These calculations were made using the program Gaussian 92 [52]; and (5) the discussion of some correlations between experimental thermodynamic parameters and calculated magnitudes using the above-mentioned theoretical methods.

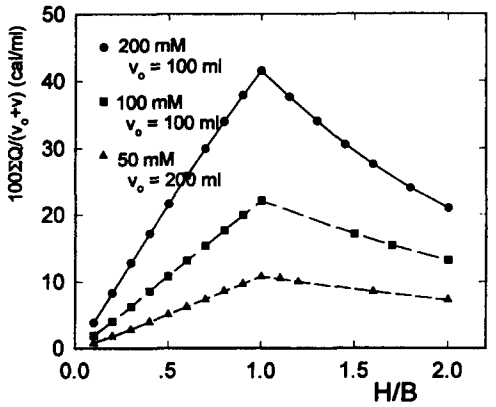

Fig. 2. Accumulative heat effect per total volume $\Sigma Q/(v_0+v)$ *vs* the ratio H/B for three enthalpy titrations in 3.0 M KCl at 25°C. The continuous lines were drawn using the partial molar enthalpies calculated in this work.

EXPERIMENTAL

The reagents and the analytical methods detailed in [35–40], the apparatus itemized in [35,38,53], the *emf* titration method described in [28,29,53] and the *enthalpy* titration method outlined in [37,40] were used. Solutions of chromate ($Z = 0$), dichromate ($Z = 1$) and hydrochloric acid of the following compositions: $S_1 = CrO_4^{2-}$ BM, K^+ 3.000 M, Cl^- $(3.000-2B)$ M, $S_2 = Cr_2O_7^{2-}$ $2B$ M, K^+ 3.000 M, Cl^- $(3.000-B)$ M, T_1 = HCl 0.1000 M, KCl 2.900 M and T_2 = HCl 1.000 M, KCl 2.000 M, respectively, were prepared. The *emf* titrations were performed at 25.00(5)°C, where known amounts of solution T_1 were successively added with a burette to the solutions S_1 or S_2, kept in an *emf* cell [28,29,53]. Likewise, the *enthalpy* titrations were carried out at 25.000(1)°C, by successive additions (v ml) of the solution T_2 from a burette to $v_0 = 100.0$ ml of the solutions S_1 or S_2 contained in the calorimeter reaction vessel [37,40].

RESULTS AND DISCUSSION

Analysis of a new series of emf *data (25°C, 3.0 M KCl)*

First, *emf* data obtained in this work will be discussed (Figs 3 and 4). In Fig. 3 the values of Z(pH, B) are given in all the interval $0 \leqslant Z \leqslant 1.16$ studied, while Fig. 4 only presents data for $Z > 1$.

In the zone $Z < 1$ the situation is very clear and the Z(pH, B) data display the expected behavior [15,35], that is the formation of the complexes $HCrO_4^-$ and $Cr_2O_7^{2-}$, that predominate at $Z = 1$. The values of the stability constant obtained were $\log\beta_{11} = 5.888(4)$, $\log\beta_{22} = 13.900(3)$ and $\log k_{22} = 2.12(1)$, with a standard deviation $\sigma(Z) = 0.002$, in good accord with the

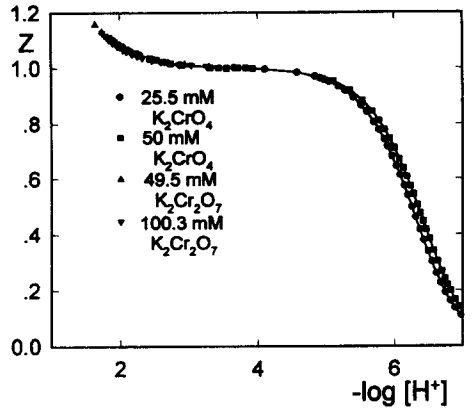

Fig. 3. Z, average number of H^+ bound per chromium(VI) at CrO_4^{2-} level *vs* pH (25°C, 3.0 M KCl). The dotted curves were calculated assuming the species $HCrO_4^-$, $Cr_2O_7^{2-}$, H_2CrO_4 and $HCr_2O_7^-$ with the stability constants $\log\beta_{11} = 5.888$, $\log\beta_{22} = 13.900$, $\log\beta_{21} = 7.004$ and $\log\beta_{32} = 15.077$, respectively.

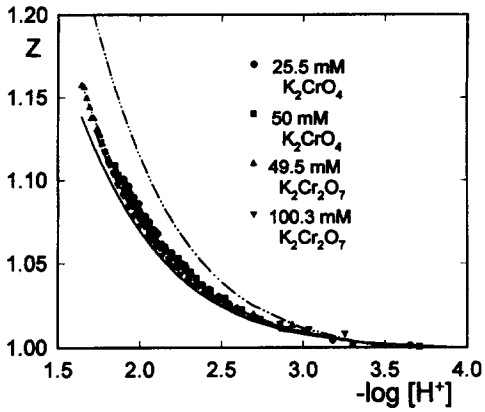

Fig. 4. Z, average number of H^+ bound per chromium(VI) at CrO_4^{2-} level *vs* pH for acid range (25°C, 3.0 M KCl). The full-draw lines were calculated assuming the species $HCrO_4^-$, $Cr_2O_7^{2-}$, H_2CrO_4 and $HCr_2O_7^-$ with the stability constants $\log\beta_{11} = 5.888$, $\log\beta_{22} = 13.900$, $\log\beta_{21} = 7.004$ and $\log\beta_{32} = 15.077$, and the heavy border and dotted border lines correspond to the *mononuclear* and the *dinuclear walls*, respectively.

earlier results, Table 1. The dotted trace curves in Fig. 3 were calculated with these stability constants.

On the other hand, for $Z > 1$, Fig. 4, data were only obtained up to $Z = 1.16$ and pH = 1.6, but unlike the results obtained by Sasaki [15], the Z(pH, B) curves, although they practically proceed together, depend on the total concentration of chromium(VI). The *heavy border* line for $B = 5\times10^{-5}$ M correspond to the *mononuclear wall* [36] above-mentioned, when only the *mononuclear* $HCrO_4^-$ and H_2CrO_4 complexes predominate, which occurs for very diluted chromium(VI) solutions. Analogously, we shall name as *dinuclear wall* the *dotted border* line for $B = 500$ mM, i.e. when only the *dinuclear* $Cr_2O_7^{2-}$ and $HCr_2O_7^-$ complexes exist, which happens to be in very strongly concentrated chromium(VI) solutions. It can be observed that as Z increases, the curves Z(pH, B) shift to the left as B decreases and the pH increases. Since at $Z = 1$ the complexes $HCrO_4^-$ and $Cr_2O_7^{2-}$ predominate, this increase in Z for pH < 3 is obviously due to the protonation of one or both species, to form the cited complexes H_2CrO_4 and $HCr_2O_7^-$, in accord with the acid–base reactions (4), estimating values of $pK \approx 1$.

$$HCrO_4^- + H^+ \overset{pK_{21}}{\rightleftarrows} H_2CrO_4$$

$$Cr_2O_7^{2-} + H^+ \overset{pK_{32}}{\rightleftarrows} HCr_2O_7^- \qquad (4)$$

However, if it is assumed that in addition to $HCrO_4^-$ and $Cr_2O_7^{2-}$ species only the acid $HCr_2O_7^{2-}$ is formed in appreciable amounts, for example, for $pK_{21} \ll 0$ and $pK_{32} = 1.0$ values, the family of curves Z(pH, B) would take the form represented in Fig. 5, where it can be seen that unlike the experimental data, as Z increases, the calculated curves are shifted towards the left as pH increases and B decreases, whereas if we assume that it forms only the complex H_2CrO_4 ($pK_{21} = 1$ and $pK_{32} \ll 0$), the family of curves Z(pH, B) would have the form observed in Fig. S1a, with a behaviour similar to that of the experimental data. Therefore, not only the $HCr_2O_7^-$ species can be expected to be formed, but also H_2CrO_4 or both complexes. Likewise, the families of curves Z(pH, B) plotted in Figs S1b–S1h were calculated supposing $pK_{21} = 1.0$, and pK_{32} varying from −1.0 to 2.0, respectively. As the value of pK_{32} increases, the *mono-* and *dinuclear walls* come closer until for $pK_{32} = 1.5$ (Fig. S1g), inversion of position takes place. Thus, from this line of argument, it can be concluded that the figure that most closely resembles Fig. 4 (experimental data) is Fig. S1c, with practically equal pK values ($pK_{21} = 1.1$ and $pK_{32} = 1.0$).

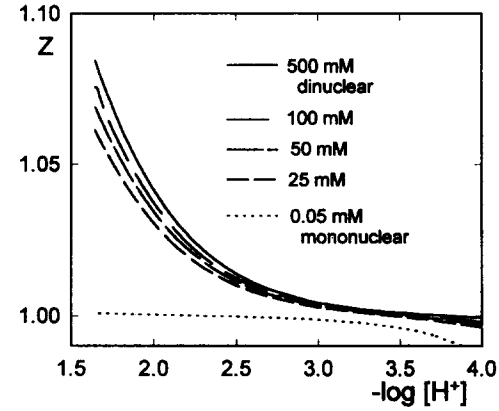

Fig. 5. Family of curves Z(pH) in the acid range were calculated assuming that the species $HCr_2O_7^-$ ($pK_{32} = 1.0$ and $pK_{11} \ll 0$) is only formed. The heavy border and dotted border lines, respectively correspond to the *mononuclear* ($B = 0.05$ mM) and the *dinuclear walls* ($B = 500$ mM).

The same conclusion is also reached supposing that for $B = 100$ mM and $B = 25$ mM, only the complexes $HCr_2O_7^-$ and H_2CrO_4, respectively were formed. Plotting the data Z(pH, 100 mM) and Z(pH, 25 mM) in accord with expressions (5a) and (5b), two straight lines were obtained with a slope ≈ 1 and ordinate in

$$\log(2Z-2)/(3-2Z) = pK_{32} - pH \qquad (5a)$$

$$\log(Z-1)/(2-Z) = pK_{21} - pH \qquad (5b)$$

the origin $pK_{32} = 1.28$ and $pK_{21} = 1.12$, respectively, Fig. S2. In conclusion, the analysis of the data $Z(\text{pH}, B) > 1$ by graphical methods indicates the formation of the complexes H_2CrO_4 and $HCr_2O_7^-$, starting from the species $HCrO_4^-$ and $Cr_2O_7^{2-}$, having similar pK values. Indeed, analysis of the data by means of version Nernst/Leta [44] of Letagrop [47], allowed the following values of stability constants to be deduced: $\log\beta_{21} = 7.004(7)$ and $\log\beta_{32} = 15.077(5)$, with a standard deviation $s(Z) = 0.002$, and values of $pK_{21} = 1.12$ and $pK_{32} = 1.18$. It should be noted that polynuclear complexes such as $Cr_3O_{10}^{2-}$ and/or $Cr_4O_{13}^{2-}$ were rejected by Letagrop. The full-draw lines of Fig. 4 were calculated using these stability constant. Finally, in Fig. 6 are presented the species distribution diagrams for $B = 50$ mM. It can be observed that the *dimers* are the more abundant species, as expected, since for $Z > 1$, the greater part of the experimental data is situated closer to the *dinuclear wall* than the *mononuclear* one (Fig. 4).

Analysis of the endothermic calorimetric data (25°C, 3.0 M in KCl) at Z > 1 using Letagrop

An analysis will be presented below of the calorimetric data with $H/B > 1$, Fig. 2 by means of the version Varm/Leta [45] of Letagrop [46]. The best fit was achieved assuming the formation of the H_2CrO_4 and $HCr_2O_7^{2-}$ complexes, in addition to $HCrO_4^-$ and $Cr_2O_7^{2-}$ predominating at $Z = 1$. The following values of the partial molar enthalpies and stability constants, in accord with [2], were obtained:

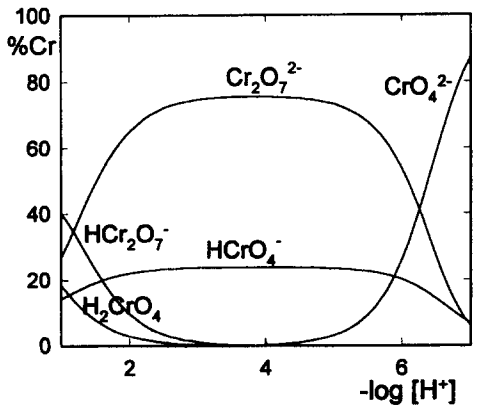

Fig. 6. Species distribution diagram as a function of pH for $B = 50$ mM in 3.0 M KCl at 25°C.

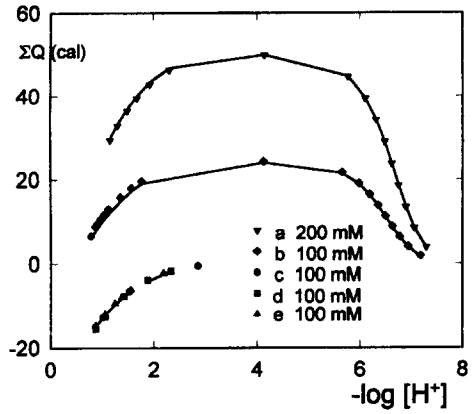

Fig. 7. Accumulative heat effect ΣQ *vs* pH for the endothermic calorimetric data (25°C, 3.0 M KCl) at $Z > 1$ and concentration in chromium(VI) B mM. Initial solutions of *a* and *b* are referred to K_2CrO_4; initial solutions of *c*, *d* and *e* are referred to $K_2Cr_2O_7$. The unbroken lines were drawn using the partial molar enthalpies determined in this work.

$\Delta H_{21} = 1.8(2)$, $\Delta H_{32} = -5.0(1)$ kcal/mol, $\log\beta_{21} = 7.56(3)$ and $\log\beta_{32} = 15.7(1)$, with $\sigma(Q) = 0.16$ cal. The experimental data are plotted in Fig. 7. The unbroken lines were calculated assuming the above parameter values.

Table 2 presents the values of the variations of free energy, enthalpy and entropy for several reactions of chromates. Because the formation of a complex is favoured by positive values of ΔS°_{pq} and negative values of ΔH°_{pq}, it can therefore be deduced that the acidification reactions of the chromates in 3.0 M KCl at 25°C is entropy-driven, since for reactions between oppositely charged ions there is a net decreasing of ioning charge, which is normally conducive to positive entropy values, as a result of a great increase on the solvent entropy when it has lost the ordenated arrangement of solvent molecules around the reagents. Contrarily, the condensation of the ion $HCrO_4^-$ to form $Cr_2O_7^{2-}$ is particularly an enthalpy-driven reaction.

On the other hand, in Table 3 we present the values of ΔG°, ΔH° and ΔS° of the stepwise acidification reactions of the ions CrO_4^{2-} and $Cr_2O_7^{2-}$, for comparative purpose with the corresponding values for molybdates(VI) and vanadates(V) [40]. In general, it can be observed that as the acid becomes stronger ΔG^0 augments, since for a molecule it is much more easy to lose H^+ as the charge decreases. Moreover, this is greatly favored by the entropy term, whereas the enthalpy term is small and unfavorable, except for the protonation of the ion $HMoO_4^-$, whose large negative enthalpy term (-11.1 kcal/mol) has been attributed to the promotion in the coordination of Mo^{VI} from four in ion $HMoO_4^-$, to six in the octahedral neutral species [54] $Mo(OH)_6$. By the way, the condensation of species $HMoO_4^-$ to form $Mo_2O_7^{2-}$ never has been observed [54]. Finally, it is noted that the successive acidification protonation of the ion CrO_4^{2-}, as well as

Table 2. Values of $\Delta G°$, $\Delta H°$ and $\Delta S°$ ($\pm 3\sigma$) for several reactions of chromates (25°C, 3.0 M K (Cl))

Reactions	ΔG^0 kcal/mol	ΔH^0 kcal/mol	ΔS^0 e.u.
$H^+ + CrO_4^{2-} \rightleftarrows HCrO_4^-$	−8.06(1)	−0.6(2)	25(1)
$2H^+ + 2CrO_4^{2-} \rightleftarrows Cr_2O_7^{2-} + H_2O$	−18.92(4)	−5.7(1)	45(1)
$2H^+ + CrO_4^{2-} \rightleftarrows H_2CrO_4$	−10.31(3)	1.8(2)	41(1)
$3H^+ + 2CrO_4^{2-} \rightleftarrows HCr_2O_7^- + H_2O$	21.4(1)	−5.0(1)	55(1)
$2HCrO_4^- \rightleftarrows Cr_2O_7^{2-} + H_2O$	−2.80(5)	−4.5(5)	−5(2)

Table 3. Values of $\Delta G°$ (kcal/mol), $\Delta H°$ (kcal/mol) and $\Delta S°$ (e.u.) for successive acid–base reactions of chromates (3.0 M K(Cl)), molybdates (1.0 M NaCl), heptamolybdates (3.0 M $Na(ClO_4)$) and decavanadates (1.0 M $Na(ClO_4)$) at 25°C [40]

	$n=$	1	2	3
$H^+ + H_{n-1}CrO_4^{n-3} \rightleftarrows H_nCrO_4^{n-2}$	$\Delta G°$	−8.06	−2.25	
	$\Delta H°$	−0.6	2.4	
	$\Delta S°$	25	16	
$H^+ + H_{n-1}Cr_2O_7^{n-3} \rightleftarrows H_nCr_2O_7^{n-2}$	$\Delta G°$	−2.5		
	$\Delta H°$	0.7		
	$\Delta S°$	11		
$H^+ + H_{n-1}MoO_4^{n-3} \rightleftarrows H_nMoO_4^{n-2}$	$\Delta G°$	−4.73	−5.1	
	$\Delta H°$	5.38	−11.1	
	$\Delta S°$	34	−20	
$H^+ + H_{n-1}Mo_7O_{24}^{n-7} \rightleftarrows H_nMo_7O_{24}^{n-6}$	$\Delta G°$	−6.0	−4.8	−3.4
	$\Delta H°$	2.6	0.8	−0.6
	$\Delta S°$	29	19	10
$H^+ + H_{n-1}V_{10}O_{28}^{n-7} \rightleftarrows H_nV_{10}O_{28}^{n-6}$	$\Delta G°$	−7.2	−5.2	−2.4
	$\Delta H°$	−8.2	1.0	0.5
	$\Delta S°$	−3	21	10

that of the $Cr_2O_7^{2-}$, is also especially enhanced by the entropy term. The diminution trend of $\Delta S°$ comes together with the anions charge decrease, which reflects the decreasing hydration of the anions as they become protonated and their charge is partially neutralized [46], except for the decavanadates where this tendency fails in the first protonation of the $V_{10}O_{28}^{6-}$ complex [40].

Analysis of the Raman spectra using Letagrop

An analysis of the Raman spectroscopy data [5,6] at the frequencies 846 and 904 cm^{-1} (Figs 8 and 9) by means of the Beer/Leta [45,50] version of Letagrop [47] assuming only $Cr_2O_7^{2-}$ [5,6] and both species $HCrO_4^-$ and $Cr_2O_7^{2-}$, respectively, is shown in Table 4. For Raman spectral measurements an expression analogous to Beer's law was assumed [55,56]. Since in the reference [5] the work was done for $B = 200$ mM, which is too high to have enough amounts of $HCrO_4^-$ due to enhanced dimerization, the fit was almost the same assuming both models (Fig. 8). However, in ref. [6], where instead the work was performed at $B = 10$ mM, the model considering both species

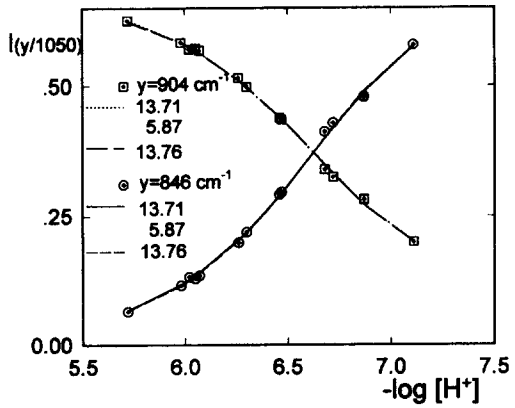

Fig. 8. Relative intensities of Raman data from Ref. [5] at frequencies 846 cm^{-1} and 904 cm^{-1} *vs* pH for $B = 200$ mM. The curves were calculated assuming the species $Cr_2O_7^{2-}$ (continuous lines), and $HCrO_4^-$ and $Cr_2O_7^{2-}$ (dotted lines) by means of Letagrop.

$HCrO_4^-$ and $Cr_2O_7^{2-}$ fits better than only supposing $Cr_2O_7^{2-}$ (Fig. 9), although the results are not sufficiently good due to the paucity of experimental

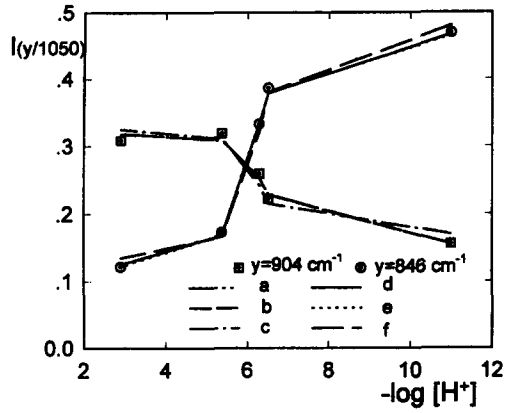

Fig. 9. Relative intensities of Raman data from Ref. [6] at frequencies 846 cm^{-1} and 904 cm^{-1} *vs* pH for $B = 10$ mM. The curves were calculated assuming the species $Cr_2O_7^{2-}$ (continuous lines), and $HCrO_4^-$ and $Cr_2O_7^{2-}$ (dotted lines) by means of Letagrop.

data. Moreover, our least-squares calculations of these data are in very good agreement with those obtained by Schwarzenbach and Meier [57].

Ab initio *calculations*

The results of the *ab initio* calculations of the energies and of the optimized geometries of the species CrO_4^{2-}, $HCrO_4^-$, H_2CrO_4 and $HCr_2O_7^-$, the existence of which in aqueous solutions has been confirmed in this work, will be discussed below. The results of the optimization of the geometries are given in Tables 5 and 6. In the case of the anion CrO_4^{2-} the results obtained in this work are compared with those obtained using another basis, in accord with references [58,59]. The values of Cr—O bond lengths calculated are in better accord with those obtained experimentally for the anion CrO_4^{2-}, using the basis set above-mentioned, and the same may be said for the anion $Cr_2O_7^{2-}$, even if these calculations present severe limitations because the basis is limited and electron correlation has not been included. It can be observed firstly that when the Cr—O bond lengths of the protonated species are compared to those of the non-protonated species, all the lengths decrease with the exception of the Cr—O distance of the oxygen bonded to the hydrogen, which increases; consequently, the OH^- group must become more labile in the substitution reactions. These results for the

Table 4. Analysis of the Raman spectroscopy data (refs [5,6]) at frequencies 846 and 904 cm^{-1} by means of Letagrop only, assuming [5,6] $Cr_2O_7^{2-}$ and both species $HCrO_4^-$ and $Cr_2O_7^{2-}$, respectively

(p,q)	$\log \beta_{pq}(3\sigma)$						
(1,1)	—	—	5.86(<6.19)	—	—	5.80(<6.10)	6.04
(2,2)	13.77[5]	13.76(5)	13.71(6)	14.5(2)[6]	14.45(<14.71)	13.78(<14.17)	13.78
B	0.2 M	—	—	0.01 M	—	—	—
μ	1.0	—	—	0.12	—	—	—
σ(I)	—	0.006	0.006	—	0.016	0.012	—
Data	Table 7 [5]			Fig. 2 [6]			Ref. [57]

Table 5. Optimized geometries (in Å and deg.) for CrO_4^{2-} and $HCrO_4^-$ species

Species	Used bases	d_{Cr-OT}	d_{Cr-OH}	∠O—Cr—O	∠Cr—O—H	Energy (a.u.)	Ref.
CrO_4^{2-}	Double-zeta val. with pseudopotentials	1.591	—	Td		−309.0614	This work
CrO_4^{2-}	3–21G	1.604	—	Td		—	[58]
CrO_4^{2-}	Minimum STO	—	—	Td		−1327.9192	[59]
CrO_4^{2-}	Extended (double-zeta)	—	—	Td		−1329.9148	[59]
CrO_4^{2-}	Experimental	1.66		Td			[58]
$HCrO_4^-$	Double-zeta val. with pseudopotentials	1.513	1.853	106.57[a] 111.93[b]	119.50	−309.81	This work
$HCrO_4^-$	Hehre's extend. bases RHF (3–21 G*)	1.537	1.794				[26]

OT = terminal oxygen, d_{Cr-OH} = chromium–oxygen distance, where the oxygen is bound to hydrogen atom.
[a] min. angle.
[b] max. angle.

Table 6. Optimized geometries (in Å and deg.) for H_2CrO_4, $Cr_2O_7^{2-}$ and $HCr_2O_7^-$ species, using double-zeta valence basis set with pseudopotentials

Species	d_{Cr-OT}	d_{Cr-OC}	d_{Cr-OH}	∠O—Cr—O	∠Cr—O—Cr	∠Cr—O—H	Energy (a.u.)	Ref.
H_2CrO_4	1.434	—	1.745	108.69[a]	—	133.51	−310.3292	This work
				110.66[b]				
$CrO_3O_7^{2-}$	1.513	1.819	—	—	139.2	—	−543.4611	[17]
$Cr_2O_7^{2-}$	1.56–1.64	1.76–1.81	—	—	122–139	—	—	Experimental, 21
$HCr_2O_7^-$	1.485	1.912	1.795	106.50[a]	162.6	123.1	−544.1636	This work
		1.628		112.00[b]				

OT = terminal oxygen, O_c = central oxygen; d_{Cr-OH} = chromium–oxygen distance, where the oxygen is bound to hydrogen atom.

[a] min. angle.

[b] max. angle.

$HCrO_4^-$ anion are in good agreement with those obtained for the anion in the crystal structure [12] of the compound $(Ph_4P)[Cr^{VI}O_3(OH)]$. Thus, three Cr—O short bond distances: 1.54, 1.55 and 1.58 Å (theoretical value 1.513 Å, Table 5) and one Cr—O (hydroxy) long bond distance: 2.02 Å (theoretical value 1.853 Å, Table 5) are found, whereas the O—Cr—O bond angles are between 106 and 113° (theoretical values lie between 106.57 and 111.93°, Table 5). The results obtained in the Mulliken population analysis, Table 7, indicate that the oxygen bonded to the proton presents a more negative charge than the remainder of the oxygens. Moreover, it can be seen in Table 5 that the anion $HCrO_4^-$ is more distorted than the species H_2CrO_4 and this in turn more than the CrO_4^{2-}, in accord with the values of the O—Cr—O bond angles calculated. Moreover, the anion $HCr_2O_7^-$ is distorted with respect to the $Cr_2O_7^{2-}$; it is also observed that the distance of the atom of chromium of the $HCrO_3$ group of the anion $HCr_2O_7^-$ to the central oxygen atom is 1.628 Å, while that of the chromium atom of the CrO_3 group of the same anion to the central oxygen atom is 1.91 Å. In the $HCr_2O_7^{2-}$ anion, the two chromium atoms have a different charge, in accord with the Mulliken population analysis calculations given in Table 7. The Cr—O—Cr angle of the anion $HCr_2O_7^-$ is 162.6°, while the same angle in the anion $Cr_2O_7^{2-}$ is between 122 and 139° [21].

Correlations between experimental thermodynamic and calculated ab initio *parameters*

It seems logical to expect the existence of direct correlations between the experimental thermodynamic parameters ($\Delta H°$, $\Delta G°$, etc.) that characterize a certain reaction and the interatomic bond models involved. Possible correlations for the acid chromates $HCrO_4^-$, $HCr_2O_7^-$ and H_2CrO_4 between some of these thermodynamic parameters and the calculated values of the bond lengths, d_{Cr-OH}, the charge of the dissociating proton, z_H and the optimized energy E, will be discussed below. Some of these magnitudes of interest are presented in Table 8. However, such correlations must be treated with caution, for two basic reasons. The first is that the calculations of molecular models are referred to non-condensed phases at 0 K, other effects having considerable influence above this temperature. The second reason is associated with the influence of the solvent since bond models generally take into account non-solvated species without taking into account the important contribution of the solvatation [60].

Although Huheey, Keiter and Keiter [61] have established that the reaction enthalpies in gaseous phase may not coincide with polar solvents as water, as can be expected in our case, the stability of the species $HCrO_4^-$ and $HCr_2O_7^-$ have been determined by us both by means of *ab initio* calculations in non-

Table 7. Atomic charges calculated through a Mulliken population analysis, using double-zeta valence basis set with pseudopotentials

CrO_4^{2-}	$HCrO_4^-$	H_2CrO_4	$Cr_2O_7^{2-}$	$HCr_2O_7^-$
Cr+1.047	+1.069	+1.204	+1.455	+1.1158 +1.2200
O_T[a] −0.762	−0.517	−0.210	−0.637	−0.4532
$O_{T'}$[a]	−0.495	−0.211	−0.660	−0.3341
O_H[b]	−0.913	−0.849		−0.8698
H	+0.373	+0.457		+0.4154
O_C[c]			−1.043	−0.8527

[a] $O_{T'}$, O_T = terminal oxygen.
[b] O_H = oxygen bound to hydrogen atom.
[c] O_c = central oxygen.

Table 8. Values of pK, $\Delta G°$, $\Delta H°$, $\Delta S°$, d_{Cr-OH}, charge z_H of the acid proton and optimized energy for the species $HCrO_4^-$, $HCr_2O_7^-$ and H_2CrO_4

	pK	$\Delta G°$ (kcal/mol)	$\Delta H°$	$\Delta S°$ (e.u.)	d_{Cr-OH} (Å)	z_H	E (a.u.)
$HCrO_4^- \rightleftarrows CrO_4^{2-} + H^+$	5.90	8.06	0.6	−25	1.853	0.373	−309.81
$HCr_2O_7^- \rightleftarrows Cr_2O_7^{2-} + H^+$	1.18	2.5	−0.7	−11	1.795	0.415	−544.16
$H_2CrO_4 \rightleftarrows HCrO_4^- + H^+$	1.12	2.2	−2.4	−16	1.745	0.457	−310.33
CrO_4^{2-}							−309.06
$Cr_2O_7^{2-}$							−543.46

condensed phase and by *emf*, calorimetric and Raman spectroscopic studies in aqueous solution. Also, for the majority of the cations hydrolytic reactions (7), where protons are split off from the water molecules bonded to the cation M^{n+}, it seems that

$$qM^{n+} + pH_2O \rightleftarrows M_q(OH)_p^{(nq-p)} + pH^+ \qquad (7)$$

the free energy change depends essentially on enthalpy. For the formation of *mononuclear* complexes the process is somewhat analogous to the dissociation of a proton from a free water molecule, for which we have $\Delta H_w \approx 13.5$ kcal/mol. For example, for the dissociation of the first proton from the ions Hg^{2+}, Fe^{2+} and Cd^{2+} the $1/p\,\Delta H^{-H}$ values are 7.2, 11.0 and 13.1 kcal/mol, respectively, reflecting the decreasing M—O bond strength in that order. Combining $1/p\,\Delta H^{-H}$ with ΔH_w, we have the enthalpy change ΔH^{OH} for the reaction (8). For many

$$qM^{n+} + pOH^- \rightleftarrows M_q(OH)_p^{(nq-p)} \qquad (8)$$

of the hydroxo complexes, $1/p\,\Delta H^{OH}$ is around −8(2) kcal/mol, except for Cd^{II} and Ni^{II} species, which have smaller values, between 0 and −3 kcal/mol [46]. Also, it has been assumed that $1/p\,\Delta G^{-H}$ could be considered as a measure of the acidity of the metallic ion, while $1/p\,\Delta H^{OH}$, except for the solvatation energy, could be taken as a measure of the M—O bond energy.

A plot of $1/p\,\Delta H^{OH}$ *vs* $1/p\,\Delta G^{OH}$ shows that all hydroxo complexes are situated on a broad band between the *isoentropic* lines $1/p\,\Delta S^{OH} \approx 10$–30 e.u. Such distributions are in agreement with *ionic model* behaviour, the more acid cations corresponding to the strongest M—O bond [30]. With this in mind, we have first plotted in Fig. S3a, the bond lengths d_{Cr-OH} *vs* the charge z_H of the proton to be dissociated: Cr—O—H^{z+}, both calculated. As expected, the charge of the proton increases as d_{Cr-OH} decreases. Secondly, the experimental values have been plotted of the enthalpy of dissociation of H^+ for the reactions (9) ΔH_{B-HB} as a function of the charge z_H of the proton to be dissociated: Cr—O—H^{z+} (Fig. S3b). Also in this case z_H increases as ΔH_{B-HB} becomes more exothermic.

$$HCrO_4^- \rightleftarrows CrO_4^{2-} + H^+$$
$$HCr_2O_7^- \rightleftarrows Cr_2O_7^{2-} + H^+$$
$$H_2CrO_4 \rightleftarrows HCrO_4^- + H^+ \qquad (9)$$

Moreover, in Fig. S3c, ΔH_{B-HB} has been plotted as a function of bond lengths d_{Cr-OH}. It is observed that d_{Cr-OH} decrease as the enthalpy become more exothermic. Lastly, there is a direct correspondence between ΔH_{B-HB} and δE_{B-HB} (calculated optimized

energies for the unprotonated species and of the protonated ones in reactions (9)). In fact, the reactions (9) become more exothermic as δE_{B-HB} decreases.

The correlation between the experimental parameter ΔH_{B-HB} and the three calculated magnitudes d_{Cr-OH}, z_H and δE_{B-HB}, is clearly manifest. It can be concluded that the ΔH_{B-HB} is an indirect measurement of the Cr—OH bond energy for the species $HCrO_4^-$, $HCr_2O_7^-$ and H_2CrO_4.

Supplementary material—Figures S1a–S1h, S2 and S3a–S3c are available from the authors on request.

Acknowledgements—We wish to thank the National Council of Scientific and Technological Research (CONICIT, Venezuela) (Project S1-1228/1981); the Council of Scientific and Humanistic Development (CDCH) of the Central University of Venezuela (UCV, Caracas) (Projects C03.05/1984 and C03.10/1986) and the Education Council of the Government of Canary Islands, Spain (Projects 14/02.06/1987, 27/08.03/1990 and 93-032/1993) for the financial support, which allowed us to build the calorimeters. L. G. Sillén of the Group of Equilibria in Solution (UCV) and R. Trujillo of the Department of Inorganic Chemistry of the University of La Laguna (ULL, Tenerife).

We also thank the Computer Center of the Faculty of Sciences (UCV), and the Interministerial Commission of Science and Technology (CICYT) for the generous gift of computer time on the Burroughs 6700, Unisys A10 and Silicon Graphics Challenger, and on the CRAY computer at CIEMAT (Madrid, Spain), respectively.

One of us (FB) is indebted to CDCH (UCV) and to the University of La Laguna (ULL) for the benefit of Studies Assistantships in the Department of Inorganic Chemistry (ULL) during 1994 and 1996, and to the CDCH (UCV) for the grant of the Unix Work Station INDY Idafe, where it carried out the last equilibrium calculations of this work.

Thanks are also due to Mrs P. Agnew and Dr Saysell for correcting the English text.

REFERENCES

1. Mazurek, W., Nichols, P. J. and West, B. O., *Polyhedron*, 1991, **10,** 753.
2. Brauer, S. L. and Wetterhahn, K. E., *J. Am. Chem. Soc.*, 1991, **113,** 3001.
3. Cotton, F. and Wilkinson, G., *Advanced Inorganic Chemistry*, 5th Edn, pp. 693–694, John Wiley & Sons, New York (1988).
4. Greenwood, N. N. and Earnshaw, A., *Chemistry of the Elements*, p. 1175, Pergamon Press, Oxford (1986).
5. Michel, G. and Machiroux, R., *J. Raman Spect.*, 1983, **14,** 22.
6. Michel, G. and Cahay, R., *J. Raman Spect.*, 1986, **17,** 79.
7. Cieslak-Golonka, M., *Coord. Chem. Rev.*, 1991, **109,** 223.
8. Cieslak-Golonka, M., *Polyhedron*, 1996, **15,** 3667.
9. Poulopoulou, V. G., Vrachnou, E., Koinis, S. and Katakis, D., *Polyhedron*, 1997, **16,** 521.
10. Palmer, D. A., Begun, G. M. and Ward, F. H., *Rev. Sci. Instrum.*, 1993, **64,** 1994.
11. Brasch, N. E., Buckingham, D. A. and Clark, C. R., *Inorg. Chem.*, 1994, **33,** 2683; *Abstract of Inorg. React. Mech. Meeting* 93, Frankfurt, 1993, 12.
12. Mukherjee, A. K. and Mukhopadhaya, A., *Acta Cryst.*, 1994, **C50,** 1401.
13. House, D. A., *Recent Developments in Chromium Chemistry. Advances in Inorganic Chemistry*, vol. 44, pp. 341–373, Academic Press Inc., London (1997).
14. Baes, C. and Mesmer, R., *The Hydrolysis of Cations*, pp. 215–257, John Wiley & Sons, New York (1976).
15. Sasaki, Y., *Acta Chem. Scand.*, 1971, **16,** 719.
16. Wilkinson, G. (Ed.), *Comprehensive Coordination Chemistry*, vol. 3, p. 943, 1256, 1259, and 1261, Pergamon Press, New York (1987).
17. Mestres, J., Duran, M., Martín-Zarza, P., Medina, E. and Gili, P., *Inorg. Chem.*, 1993, **32,** 4708.
18. Jackson, J. and Taube, H., *J. Phys. Chem.*, 1965, **69,** 1844.
19. Pladziewicz, J. and Espenson, J., *Inorg. Chem.*, 1971, **10,** 634.
20. Pope, M. T., *Heteropoly and Isopoly Oxometalates*, pp. 42 and 48, Springer–Verlag, Berlin (1983).
21. Martín-Zarza, P., Gili, P., Rodríguez-Romero, F. V., Ruíz-Pérez, C. and Solans, X., *Polyhedron*, 1995, **14,** 2907.
22. Lofgren, P., *Acta Cryst.*, 1973, **B29,** 2140; *Chem. Scripta*, 1974, **5,** 91.
23. Lorenzo-Luis, P. A., Martín-Zarza, P., Gili, P., Arrieta, J. M., Germain, G. and Dupont, L., *Eur. J. Sol. State and Inorg. Chem.*, 1995, **32,** 353.
24. Wolfsberg, M. and Helmholtz, *J. Chem. Phys.*, 1952, **20,** 83.
25. Salahub, D. and Zerner, M. C., *The Challenge of d and f Electrons: Theory and Computation*, ACS Symposium Series 394, American Chemical Society, Washington DC (1989).
26. Martín-Zarza, P., Gili, P., Ruíz-Pérez, C., Rodríguez-Romero, F. V., Lotter, G., Arrieta, J. M., Torrent, M., Mestres, J., Sola, M. and Durán, M., *Inorg. Chim. Acta*, 1997, **258,** 53.
27. Ozeki, T., Kinoshita, Y., Adachi, H. and Ikeda, S., *Bull. Chem. Soc. Japan*, 1994, **67,** 1041.
28. Ingri, N. and Brito, F., *Acta Chem. Scand.*, 1959, **13,** 1971.
29. Brito, F., *An. Quím.*, 1966, **62B,** 13.
30. Brito, F., Ascanio, J., Gonçalves, J. M. and Franceschetto, M., *An. Quím.*, 1983, **79B,** 319.
31. Owen, J. and King, L., *J. Am. Chem. Soc.*, 1943, **65,** 1612.
32. Biedermann, G. and Sillén, L. G., *Arkiv Kemi*, 1952, **5,** 425.
33. Sillén, L. G., *Master Variables and Activity Scales, Advances in Chemistry Series*, American Chemical Society, 1967, **67**(3), 45.
34. MacInnes, D. and Longworth, *Trans. Electrochem. Soc.*, 1937, **71,** 73.
35. Hernández, C., *Equilibrium and Kinetic Study of the Chromate–Dichromate System* (25°C *and* 3.0 *M KCl*), Lic. Thesis, Faculty of Sciences, UCV, Caracas, Venezuela (1968).
36. Biedermann, G. and Sillén, L. G., *Acta Chem. Scand.*, 1956, **10,** 1011.

37. Brito, F., Ascanio, J. and Franceschetto, M., *An. Quím.*, 1974, **70,** 465.
38. Ascanio, J. and Brito, F., *An. Quím.*, 1973, **69,** 177.
39. Ascanio, J., Ph.D. Thesis, Faculties of Science, UCV, Venezuela and ULL, Tenerife, Spain (1975).
40. Araujo, L., Ph.D. Thesis, Faculty of Science, UCV, Caracas, Venezuela (1991).
41. Alvarado, C., Lic. Thesis, Faculty of Science, UCV, Venezuela (1974).
42. Brito, F., Ascanio, J., Mateo, S., Hernández, C. and Alvarado, E., to be published.
43. Brito, F. and Gonçalves, J., *Project S*1-1228, CONICIT, Caracas (1981).
44. Brito, F., Mederos, A., Gili, P., Domínguez, S. and Martín-Zarza, P., *J. Coord. Chem.*, 1988, **17,** 311.
45. Brito, F., *Project* 14/02.06.87, Gobierno de Canarias (1987).
46. Arnek, R., *Arkiv Kemi*, 1970, **32,** 81, 55.
47. Ingri, N. and Sillén, L. G., *Arkiv Kemi*, 1964, **23,** 97, and Sillén, L. G., Warnqvist, B., Arnek, R., Wahlberg, O., Brauner, P. and Whiteker, R., *Arkiv Kemi*, 1969, **31,** 315, 344, 353 and 365.
48. Muldrow, C. and Hepler, L., *J. Am. Chem. Soc.*, 1957, **79,** 4045.
49. Hepler, L., *J. Am. Chem. Soc.*, 1958, **80,** 6181.
50. Sillén, L. G. and Warnqvist, B., *Arkiv Kemi*, 1969, **31,** 377.
51. Hay, P. and Wadt, W., *J. Chem. Phys.*, 1985, **82,** 270; 1985, **82,** 299.
52. Gaussian 92, Revision, Frisch, A. M. J., Trucks, G. W., Head-Gordon, M., Gill, P. W., Wong, M. W., Foresman, J. B., Johnson, B. G., Schlegel, H. B., Robb, M. A., Replogle, E. S., Gomperts, R., Andres, J. L., Raghavachari, K., Binkley, J. S., Gonzalez, C., Martin, R. L., Fox, D. J., Defrees, D. J., Baker, J., Stewart, J. J. P., Pople, J. A., Gaussian, Inc. Pittsburgh PA (1992).
53. Mederos, A., Gili, P., Domíguez, S., Benítez, A., Palacios, M. S., Hernández, M., Martín, P., Rodríguez, M., Ruíz, C., Lahoz, F., Oro, L., Brito, F., Arrieta, J. M., Vlassi, M. and Germain, G., *J. Chem. Soc., Dalton Trans.*, 1990, 1477.
54. Cruywagen, J. and Rohwer, E., *Inorg. Chem.*, 1975, **14,** 3136.
55. Jarv, T., Bulner, J. and Trish, D., *J. Phys. Chem.*, 1967, **81,** 649.
56. Sharvell, H. and Bukner, J., *Vibrational Spectra and Structure*, J. R. During, Ed., Elsevier, New York (1977).
57. Schwarzenbach, G. and Meier, J., *J. Inorg. Nucl. Chem.*, 1958, **8,** 302.
58. Dobbs, K. and Hehre, W., *J. Comp. Chem.*, 1987, **8,** 861.
59. Connor, J., Hillier, J., Saunders, V., Wood, M. and Barber, M., *Mol. Phys.*, 1972, **24,** 497.
60. Phillips, C. S. G. and Williams, R. J. P., *Inorganic Chemistry*, Vol. 1, pp. 251–252, Oxford University Press, London (1965).
61. Huheey, J., Keiter, E. and Keiter, R., *Inorganic Chemistry. Principles of Structure and Reactivity*, pp. 330–344, Harper & Row Pub., New York, 4th Edn (1993).